UGC Approved Journal

IARJSET

ISSN (Online) 2393-8021
ISSN (Print) 2394-1588

International Advanced Research Journal in Science, Engineering and Technology

ISO 3297:2007 Certified

Vol. 4, Issue 9, September 2017

Neuro Fuzzy based Active Filter for Performance Analysis of DFIG

A. Bala Subrahmanyam[1], B. Srinivasaraju[2]

Student, Vignan's Lara Institute of Technology and Sciences, Guntur, Vadlamudi[1]

Assistant Professor, Vignan's Lara Institute of Technology and Sciences, Guntur, Vadlamudi[2]

Abstract: This paper proposes the operation of doubly fed induction generator (DFIG) with an integrated active filter capabilities by using grid-side converter (GSC). The wind energy conversion system acts as a static compensator (STATCOM) for supplying harmonics even when the wind turbine is in shutdown condition. Compared to the multiple regression analysis neuro fuzzy logic showed higher accuracy in prediction for the five outputs studied. The important role in the grid side converter is supplying harmonics in addition to its slip power transfer. The rotor-side converter (RSC) is used for gaining maximum power extraction and also to supply required reactive power to the DFIG. Control algorithms of both GSC and RSC are presented in detail . Here we are using the neuro fuzzy controller compared to other controllers because of its accurate performance. The proposed DFIG- based WECS is simulated using MATLAB/Simulink.

Index Terms: Neuro fuzzy controller, Doubly fed induction generator (DFIG), integrated active filter, nonlinear load, power quality, wind energy conversion system(WECS).

NOMENCLATURE

v_{ab}, v_{bc}, v_{ca}	Three phase stator voltages.
i_{sa}, i_{sb}, i_{sc}	Three phase stator currents.
i_{ra}, i_{rb}, i_{rc}	Three phase rotor currents.
i_{ga}, i_{gb}, i_{gc}	Three phase grid currents.
i_{la}, i_{lb}, i_{lc}	Three phase load currents.
$i_{\text{gsc}a}, i_{\text{gsc}b}, i_{\text{gsc}c}$	Three phase grid-side convertor (GSC) currents.
i_{dr}	Direct axis rotor current.
i_{qr}	Quadrature axis rotor current.
$\widetilde{i_{ld}}$	Direct axis load current.
$\overline{i_{ld}}$	Direct axis fundamental load current.
P_g	Active power fed to the grid.
Q_g	Reactive power fed to the grid.
P_s	Stator active power.
Q_s	Stator reactive power.
Q_s	Stator reactive power.
P_l	Load active power.
Q_l	Load reactive power.

1. INTRODUCTION

Nowaday's non renewable energy resources are getting degrading and also environmental pollution problems are arising. And power demand also going on increasing by the increasing level of utility of power So the renewable sources are being utilized to meet the ever increasing energy demand. The cost of non renewable energy resources are increasing due to a relatively low-cost of electricity production wind energy is taken into account to be one amongst the potential sources of fresh energy for the long run. The study owes and also the associated controllers area unit, thus, turning into a lot of and a lot of important with every passing day. Nowadays, several complete loads area unit powered by renewable supply of energy. And controlling of this project is completed by using neuro fuzzy controller.

The other main advantages of this renewable source are eco-friendliness and unlimited in nature. Therefore, the wind energy is that the most preferred out of all renewable energy sources. in the initial days, wind turbines are used as fixed speed wind turbines with squirrel cage induction generator and condenser banks. Most of the wind

UGC Approved Journal

IARJSET

ISSN (Online) 2393-8021
ISSN (Print) 2394-1588

International Advanced Research Journal in Science, Engineering and Technology

ISO 3297:2007 Certified

Vol. 4, Issue 9, September 2017

turbines are fixed speed due to their simplicity and low price. By perceptive turbine characteristics, one will clearly determine that for extracting most power, the machine should run at variable rotor speeds at completely different wind speeds. using trendy power electronic converters, the machine is able to run at adjustable speeds. Out of all variable speed wind turbines, doubly fed induction generators (DFIGs) are preferred due to their low price. the other advantages of this DFIG are the higher energy output, lower convertor rating, and better utilization of generators. These DFIGs additionally provide good damping performance for the weak grid. independent control of active and reactive power is achieved by the decoupled vector control algorithm given in and. This vector control of such system is usually realized in synchronously rotating reference frame destined in either voltage axis or flux axis. during this work, the control of rotor-side convertor (RSC) is implemented in voltage-oriented reference system. Grid code necessities for the grid connection and operation of wind farms are mentioned in. Response of DFIG-based

TABLE I CURRENT DISTORTION LIMITS FOR GENERAL DISTRIBUTION S YSTEMS IN TERMS OF INDIVIDUAL HARMONICS ORDER (ODD HARMONICS)

I_{sc}/I_L	<11	11 ≤ h ≤17	17 ≤ h ≤ 23	23 ≤ h ≤ 35	35 ≤ h	TDD
< 20	4.0	2.0	1.5	0.6	0.3	5.0
20 < 50	7.0	3.5	2.5	1.0	0.5	8.0
50 < 100	10	4.5	4.0	1.5	0.7	12
100 < 1000	12	5.5	5.0	2.0	1.0	15.0
> 1000	15.0	7.0	6.0	2.5	1.4	20.0

Maximum harmonic current distortion is in percent of IL. Isc = maximum short-circuit current at PCC; IL = maximum demand load current (fundamental frequency component) at PCC.

wind energy conversion system (WECS) to grid disturbance is compared to the fixed speed WECS in. as the wind penetration in the grid becomes significant, the utilization of variable speed WECS for supplementary jobs like power smoothening and harmonic mitigation are compulsory additionally to its power generation. This power smoothening is achieved by as well as super magnetic energy storage systems as proposed in. the other auxiliary services like reactive power requirement and transient stability limit are achieved by including static compensator (STATCOM) in.

A distribution STATCOM (DSTATCOM) let alone fly-wheel energy storage system is employed at the wind farm for mitigating harmonics and frequency disturbances. However, the authors have used 2 a lot of additional converters for this purpose. a super condenser energy storage system at the dc link of unified power quality conditioner (UPQC) is proposed in for improving power quality and reliability. in all above methods , the authors have used separate converters for compensating the harmonics and also for controlling the reactive power. However, in later stages, some of the researchers have changed the control algorithms of already existed DFIG converters for mitigating the power quality issues and reactive power compensation

A distribution STATCOM (DSTATCOM) let alone fly-wheel energy storage system is employed at the wind farm for mitigating harmonics and frequency disturbances. However, the authors have used 2 a lot of additional converters for this purpose. a super condenser energy storage system at the dc link of unified power quality conditioner (UPQC) is proposed in for improving power quality and reliability. in all above methods , the authors have used separate converters for compensating the harmonics and also for controlling the reactive power. However, in later stages, some of the researchers have changed the control algorithms of already existed DFIG converters for mitigating the power quality issues and reactive power compensation.

By using RSC reactive power compensation and harmonic compensation is obtained. Therefore, harmonics are injected from the RSC into the rotor windings. which creates losses and noise in the machine. These totally different harmonics in rotating part may also produce mechanical unbalance. These methods increase the RSC rating. In and, harmonic compensation and reactive power control are done using GSC. Therefore, the harmonics are not passing through machine windings in all these cases.in this work, a new control algorithm for GSC is planned for compensating harmonics produced by nonlinear loads using an indirect current control. RSC is used for controlling the reactive power of DFIG. And PWM pulses are generated without any error by exploitation the fuzzy controller the opposite main advantage of planned DFIG is that it works as an energetic filter even once the turbine is in shutdown condition. Therefore, it compensates load reactive power and harmonics at turbine stall case. The dynamic performance of the planned DFIG is additionally in contestable for varied wind speeds and changes in unbalanced nonlinear hundreds at purpose of common coupling (PCC).

UGC Approved Journal

IARJSET

ISSN (Online) 2393-8021
ISSN (Print) 2394-1588

International Advanced Research Journal in Science, Engineering and Technology

ISO 3297:2007 Certified

Vol. 4, Issue 9, September 2017

II. SYSTEM CONFIGURATION AND OPERATING PRINCIPLE

In DFIG, the stator coil is directly connected to the grid as shown in Fig. 1. Fig. 1 shows a schematic diagram of the planned DFIG primarily based WECS with integrated active filter capabilities. 2 back-to-back connected voltage source converters (VSCs) are placed between the rotor and thus the grid. nonlinear loads are connected at PCC as shown in Fig. 1. The planned DFIG works as an active filter additionally to the active power generation similar to traditional DFIG.

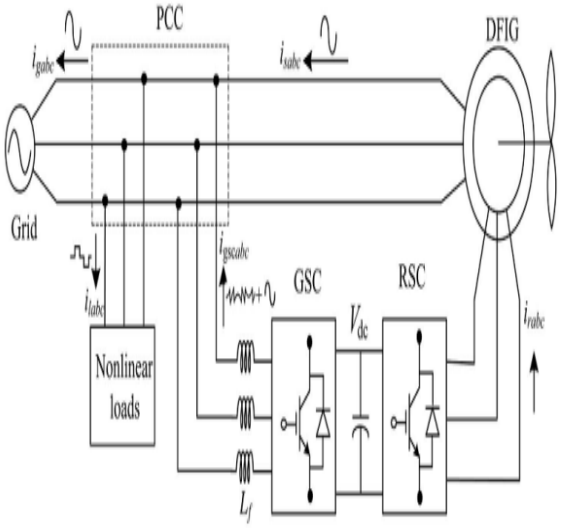

Fig. 1. Proposed system configuration

Harmonics generated by the nonlinear load connected at the PCC distort the PCC voltage. These nonlinear load harmonic currents are mitigated by GSC control, that the stator coil and grid currents are harmonic-free. RSC is controlled for achieving maximum power point tracking (MPPT) and additionally for creating unity power factor at the stator coil aspect victimization voltage-oriented reference frame. Synchronous reference frame (SRF) control methodology is used for extracting the fundamental component of load currents for the GSC control.

III. DESIGN OF DFIG-BASED WECS

Selection of ratings of VSCs and dc-link voltage is extremely much important for the successful operation of WECS. The ratings of DFIG and dc machine used in this experimental system are given in Appendix. in this section, a detailed style of VSCs and dc-link voltage is discussed

A .Selection of DC-Link Voltage

The selection of dclink voltage depends on both rotor voltage and PCC voltage. while considering from the rotor side, the rotor voltage is slip times the stator voltage. DFIG used in this prototype has stator to rotor turns ratio as 2:1. Normally, the DFIG operating slip is ±0.3. So, the rotor voltage is always less than the PCC voltage. So, the design criteria for the selection of dc-link voltage is achieved by considering only PCC voltage. While considering.

From the GSC side, the PCC line voltage (v a b) is 230 V, as the machine is connected in delta mode. Therefore, the dc-link voltage is estimated as

$$V_{dc} \geq \frac{2\sqrt{2}}{\sqrt{3}*m} V_{ab} \qquad (1)$$

where Va b is the line voltage at the PCC. Maximum modulation index is selected as 1 for linear range. The value of dc-link voltage (Vdc) by (1) is estimated as 375 V. Hence, it is selected as 375V.

A. Selection of VSC Rating

The lagging volt-ampere reactive (VAR) was draws by DFIG for its excitation to build the rated air gap voltage. It is calculated from the machine parameters that the lagging VAR of 2 kVAR is needed when it is running as a motor. In DFIG case, the operating speed range is 0.7 to 1.3 p.u. Therefore, the maximum slip (smax) is 0.3. reactive power of 600 VAR (Smax ∗ Qs= 0.3 ∗ 2 kVAR) is needed from the rotor side (Q rmax) For making unity power factor at the stator side. The maximum rotor active power is (Smax ∗ P). The power rating of the DFIG is 5 kW. Therefore,

UGC Approved Journal
IARJSET
ISSN (Online) 2393-8021
ISSN (Print) 2394-1588
International Advanced Research Journal in Science, Engineering and Technology
ISO 3297:2007 Certified
Vol. 4, Issue 9, September 2017

the maximum rotor active power (Prmax) is 1.5 kW (0.3 ∗ 5 kW = 1.5 kW). So, the rating of the VSC used as RSC Srated is given as

$$S_{rated} = \sqrt{P_{r\,max}^2 + Q_{r\,max}^2} \quad (2)$$

Thus, kVA rating of RSC Srated is calculated as 1.615 kVA.

B. Design of Interfacing Inductor

The design of interfacing inductors between GSC and PCC depends upon allowable GSC current limit (igscpp), dc-link voltage, and switching frequency of GSC. Maximum possible GSC line currents are used for the calculation. Maximum line current depends upon the maximum power and the line voltage at GSC. The maximum possible power in the GSC is the slip power. In this case, the slip power is 1.5 kW. Line voltage (VL) at the GSC is 230 V (the machine is connected in delta mode). So, the line current is obtained as I gsc = 1.5 kW/(√3 ∗ 230) = 3.765 A. Considering the peak ripple current as 25% of rated GSC current, the inductor value is calculated as

$$L_i = \frac{\sqrt{3} m v_{dc}}{12 a f_m \Delta i_{gsc}} = \frac{\sqrt{3}\times 1\times 375}{12\times 1.5\times 10000\times 0.25\times 3.76} = 3.8\text{mH}. \quad (3)$$

Interfacing inductor between PCC and GSC is selected as 4 mH.

IV. CONTROL S TRATEGY AND SIMULATION RESULTS

Control algorithms for both GSC and RSC are presented in this section. Complete control schematic is given in Fig. 2. The control algorithm for emulating wind turbine characteristics using dc machine and Type A chopper is also shown in Fig. 2.

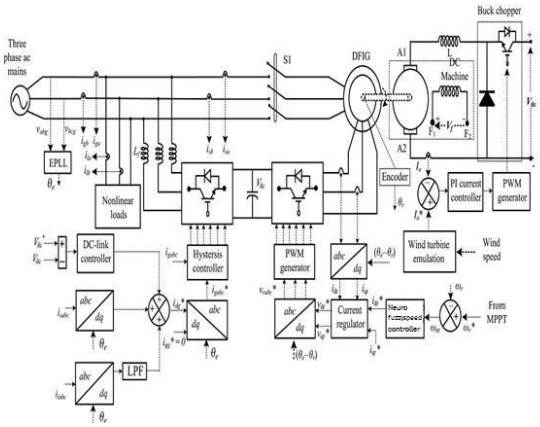

Fig. 2. Control algorithm of the proposed WECS.

A. Control of RSC

Direct axis reference rotor current is selected such that maximum power is extracted for a particular wind speed. This can be achieved by running the DFIG at a rotor speed for a particular wind speed. Therefore, the outer loop is selected as a speed controller for

$$i_{dr}^*(k) = i_{dr}^*(k-1) + k_{pd}\{\omega_{er}(k) - \omega_{er}(k-1)\} + k_{id}\,\omega_{er}(k) \quad (4)$$

where the speed error (ωer) is obtained by subtracting sensed speed (ωr) from the reference speed (ωr∗). kpd and kid are the proportional and integral constants of the speed controller. ω er(k) and ωer(k − 1) are the speed errors at kth and (k−1)th instants. i* dr(k) and i*dr(k − 1) are the direct axis rotor reference current at kth and (k−1)th instants. Reference rotor speed (ωr∗) is estimated by optimal tip speed ratio control for a particular wind speed.

Here, the RSC is controlled in voltage-oriented reference frame. Therefore, the active and reactive powers are controlled by controlling direct and quadrature axis rotor currents (idr and iqr), respectively. achieving direct axis reference rotor current (i∗dr) as Inner current control loops are taken for control of actual direct and quadrature axis rotor currents (idr and iqr) close to the direct and quadrature axis reference rotor currents (i∗dr and i∗ qr). The rotor currents idr and iqr are calculated from the sensed rotor currents (ira, irb, and irc) as

$$i_{dr} = 2/3\left[i_{ra}\sin\theta_{slip} + i_{rb}\sin(\theta_{slip} - 2\pi/3) + i_{rb}\sin(\theta_{slip} - 2\pi/3)\right] \quad (5)$$

$$i_{qr} = 2/3\left[i_{ra}\cos\theta_{slip} + i_{rb}\cos(\theta_{slip} - 2\pi/3) + i_{rb}\cos(\theta_{slip} - 2\pi/3)\right] \quad (6)$$

where slip angle (θslip) is calculated as

$$\theta_{slip} = \theta_e - \theta_r \quad (7)$$

UGC Approved Journal

IARJSET

ISSN (Online) 2393-8021
ISSN (Print) 2394-1588

International Advanced Research Journal in Science, Engineering and Technology

ISO 3297:2007 Certified

Vol. 4, Issue 9, September 2017

where θ e is calculated from PLL for aligning rotor currents into voltage axis. The rotor position (θr) is achieved with an encoder.

Direct and quadrature axis rotor voltages (vdr and vqr) are obtained from direct and quadrature axis rotor current errors (ider and iqer) as

$$v'_{dr}(k) = v'_{dr}(k-1) + k_{pdv}\{i_{der}(k) - i_{der}(k-1)\} + k_{idv}\, i_{der}(k) \quad (8)$$

$$v'_{qr}(k) = v'_{qr}(k-1) + k_{pdv}\{i_{qer}(k) - i_{qer}(k-1)\} + k_{iqv}\, i_{qer}(k) \quad (9)$$

Where

$$i_{der} = i^*_{dr} - i_{dr} \text{ and } i_{qer} = i^*_{qr} - i_{qr} \quad (10)$$

where k pdv and kidv are the proportional and integral gains of direct axis current controller. K pqv and kiqv are the proportional and integral gains of quadrature axis current controller. Direct and quadrature components are decoupled by adding some compensating terms as

$$v^*_{dr} = v'_{dr} + (\omega_e - \omega_r)\sigma L_r i_{dr} \quad (11)$$

$$v^*_{qr} = v'_{qr} - (\omega_e - \omega_r)(L_m i_{dr} + \sigma L_r i_{dr}) \quad (12)$$

These reference direct and quadrature voltages (vdr∗ , vqr∗) are converted into three phase reference rotor voltages (vra∗ , vrb∗ , vrc∗) as

$$v^*_{ra} = v^*_{dr} \sin\theta_{slip} + v^*_{qr} \cos\theta_{slip} \quad (13)$$

$$v^*_{rb} = v^*_{dr} \sin(\theta_{slip} - 2\pi/3) + v^*_{qr} \cos(\theta_{slip} - 2\pi/3) \quad (14)$$

$$v^*_{rc} = v^*_{dr} \sin(\theta_{slip} - 2\pi/3) + v^*_{qr} \cos(\theta_{slip} - 2\pi/3) \quad (15)$$

These three phase rotor reference voltages (vra∗ , vrb∗ ,vrc∗) are compared with triangular carrier wave of fixed switching frequency for generating pulse-width modulation (PWM) signals for the RSC.

The tuning of fuzzy controllers used in both RSC and GSC are achieved using Ziegler Nichols method. Initially, kid value is set to zero and the value of k pd was increased until the response stars oscillating with a period of Ti. Now, the value of kpd is taken as 0.45 k pd and kid is taken as 1.2 kpd/Ti.

Normally, the quadrature axis reference rotor current (i∗qr) is selected such that the stator reactive power (Q s) is made zero. In this DFIG, quadrature axis reference rotor current (i∗qr) is selected for injecting the required reactive power.

B. Control of GSC

The novelty of this work lies in the control of this GSC for mitigating the harmonics produced by the nonlinear loads.

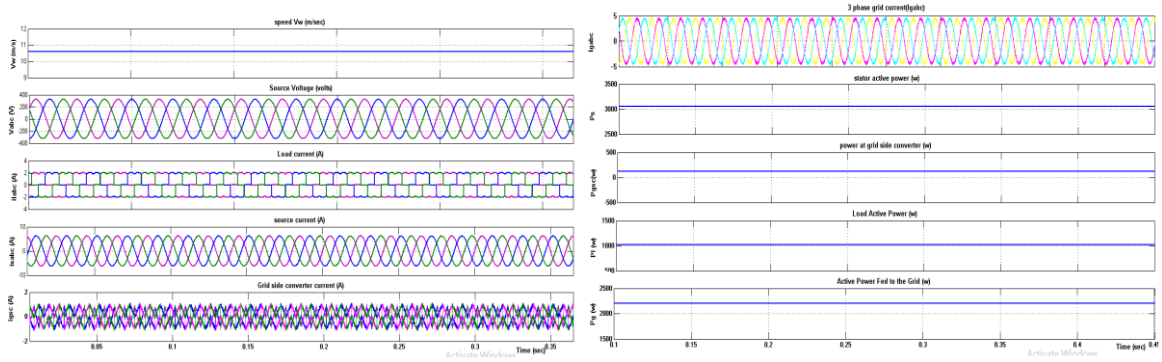

Fig. 3. Simulated performance o f the proposed DFIG-based W ECS at fixed wind speed of 10.6m/s (rotor speed of 1750rpm).

The control block diagram of GSC i s shown in Fig. 2. Here, an indirect current control i s applied on t he grid currents f or making them sinusoidal and balanced. Therefore, this GSC s upplies t he harmonics for making grid currents s inusoidal and balanced. Active power component of GSC current is obtained by processing the dc-link voltage error (vdce) between reference and estimated dc-link voltage (Vdc∗ and Vdc) through fuzzy controller as

$$i^*_{gsc}(k) = i^*_{gsc}(k-1) + k_{pdc}\{v_{dce}(k) - v_{dce}(k-1)\} + k_{idc}\, v_{dce}(k) \quad (16)$$

where kpdc and kidc are proportional and integral gains of dc-link voltage controller. Vdce(k) and Vdce(k − 1) are dclink voltage errors at kth and (k−1)th instants. i∗gsc(k) and i∗gsc(k − 1) are active power component of GSC

UGC Approved Journal

IARJSET

ISSN (Online) 2393-8021
ISSN (Print) 2394-1588

International Advanced Research Journal in Science, Engineering and Technology

ISO 3297:2007 Certified

Vol. 4, Issue 9, September 2017

current at kth and (k−1)th instants. Active power component of stator current (ids) is obtained from the sensed stator currents (isa, isb, and isc) using abc to dq transformation as

$$i_{ds} = 2/3\,[i_{sa}\,sin\,\theta_e + i_{sb}\,sin(\theta_e - 2\pi/3) + i_{sc}\,sin(\theta_e + 2\pi/3)] \quad (17)$$

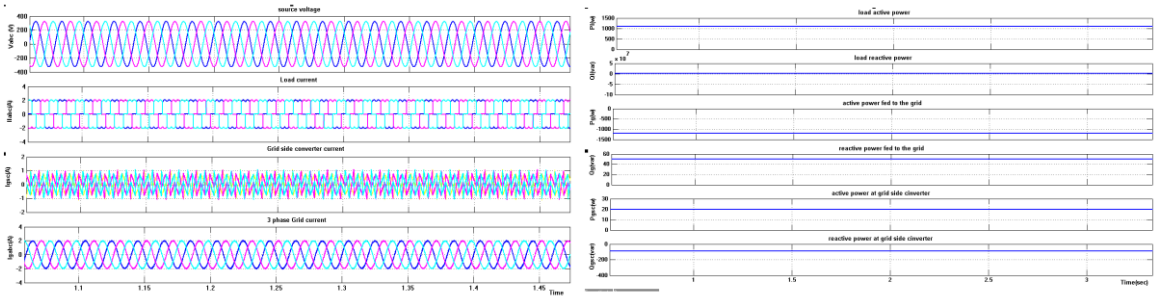

Fig. 4. Simulated performance of the proposed DFIG-based WECS working as a STATCOM at zero wind speed

Fundamental active load current (ild) is obtained using SRF theory. Instantaneous load currents (ilabc) and the value of phase angle from EPLL are used for converting the load currents in to synchronously rotating dq frame (ild). In synchronously rotating frames, fundamental frequency currents are converted into dc quantities and all other harmonics are converted into non-dc quantities with a frequency shift of 50 Hz.

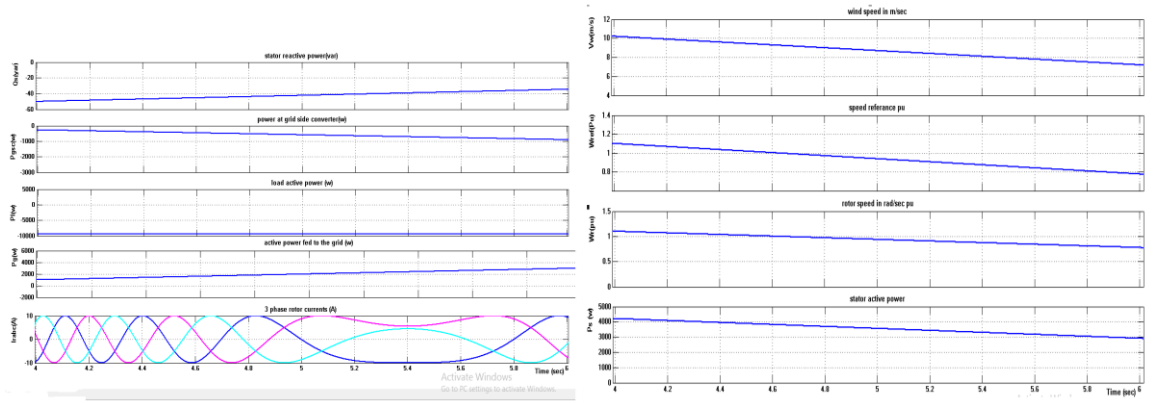

Fig. 5. Simulated performance of proposed DFIG for fall in wind speed

load current (ild) in synchronously rotating frame and the loss component of GSC current (i∗gsc) as

$$i^*_{gd} = i^*_{gsc} + i_{ds} - \overline{i_{ld}} \quad (18)$$

DC values of load currents in synchronously rotating dq frame (ild) are extracted using low-pass filter (LPF). Direct axis component of reference grid current (i∗gd) is obtained from the direct axis current of stator current (ids) and Quadrature axis component of reference grid current (i∗gq) is selected as zero for not to draw any reactive power from grid. The hysteresis current controller is used to generate switching pulses for the GSC. The hysteresis controller is a feedback current control where sensed current tracks the reference current within a hysteresis band (ihb) [34]. At every sampling instant, the actual current (igabc) is compared to the reference current (i∗gabc) as

$$\Delta i_{gabc} = i^*_{gabc} - i_{gabc} \quad (19)$$

$$\text{When} \quad \Delta i_{gabc} > i_{hb} \text{ lower switch is turned ON} \quad (20)$$

$$\text{When } \Delta i_{gabc} > i_{hb}\text{, upper switch is turned ON.} \quad (21)$$

Using these equations, gating pulses for three phases of GSC are generated in the same way.

Neuro fuzzy

In the field of artificial intelligence, neuro-fuzzy refers to combinations of artificial neural networks and fuzzy logic. Neuro-fuzzy was proposed by J. S. R. Jang. Neuro-fuzzy hybridization results in a hybrid intelligent system that synergizes these two techniques by combining the human-like reasoning style of fuzzy systems with the learning and connectionist structure of neural networks. Neuro-fuzzy hybridization is widely termed as Fuzzy Neural Network (FNN) or Neuro-Fuzzy System (NFS) in the literature.

UGC Approved Journal

IARJSET

ISSN (Online) 2393-8021
ISSN (Print) 2394-1588

International Advanced Research Journal in Science, Engineering and Technology

ISO 3297:2007 Certified

Vol. 4, Issue 9, September 2017

Neuro fuzzy has many advantages i.e it can be stated that the normalized error obtained from neurofuzzy logic was lower. Compared to the multiple regression analysis neurofuzzy logic showed higher accuracy in prediction for the five outputs studied. Rule sets generated by neurofuzzy logic are completely in agreement with the findings based on statistical analysis and advantageously generate understandable and reusable knowledge. Neurofuzzy logic is easy and rapid to apply and outcomes provided knowledge not revealed via statistical analysis. the most important advantage of neural networks is their adaptivity. Neural networks can automatically adjust their weights to optimize their behavior as pattern recognizers, decision makers, system controllers, predictors, etc.

In this paper a neuro-fuzzy control strategy, for each of the input, four fuzzy subsets have been employed. These are ZE (zero), L (low), M (medium) and H (high). So for all of these fuzzy sets, a gaussian membership function has been used. As each of the two inputs has four subsets, there are altogether 16 control rules in the neuro-fuzzy logic controller.

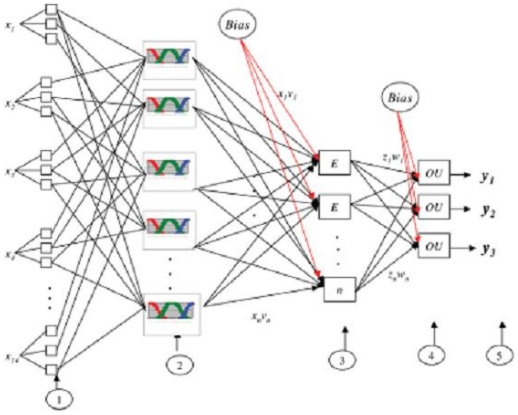

Fig. 9 A network of nodes using neuro-fuzzy integrated approach.

VI. RESULTS AND DISCUSSION

Both simulated results are presented in this section for validating steady-state and dynamic performances of this proposed DFIG with integrated active filter capabilities.

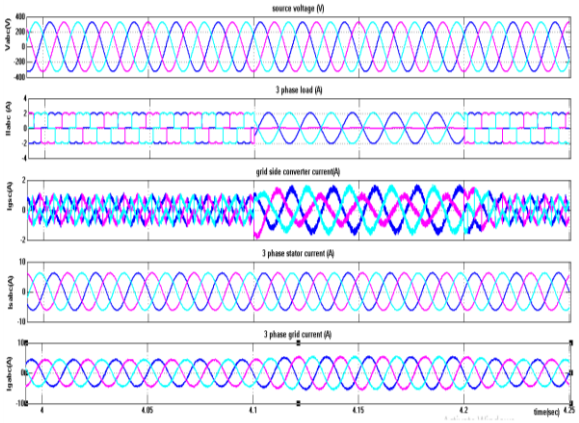

Fig. 8. Dynamic performance of DFIG-based WECS for the sudden removal and application of local loads.

VII. CONCLUSION

This projected DFIG, the reactive power for the induction machine has been provided from the RSC and the load reactive power has been supplied from the GSC The grid side device control algorithm of this DFIG has been changed for supplying the harmonics and reactive power of the local loads.. both active and reactive powers has been achieved by RSC control. The controlling for this device is completed by the neuro fuzzy controller The projected DFIG has additionally been verified at turbine obstruction condition for compensating harmonics and reactive power of local loads. This proposed system with an integrated active filter has been simulated using MATLAB/Simulink environment Dynamic performance of this proposed GSC control algorithm has also been verified for the variation in the wind speeds and for local nonlinear load.

UGC Approved Journal

IARJSET

ISSN (Online) 2393-8021
ISSN (Print) 2394-1588

International Advanced Research Journal in Science, Engineering and Technology

ISO 3297:2007 Certified

Vol. 4, Issue 9, September 2017

APPENDIX

1) DFIG: 3.7 kW, $R_s = 1.32$ ohm, $L_{ls} = 6.832$ mH, $R_2 = 1.708$ ohm, $L_{lr} = 6.832$ mH, $R_m = 419.646$ ohm, $L_m = 0.219$ H, $J = 0.1878$ kg $\cdot m^2$, stator to rotor turns ratio $N_r/N_s = 1/2$, stator rated rms current = 12 A, rotorrated rms current = 18 A.
2) DC machine: $R_a = 1.3$ ohms, $R_f = 220$ ohms, $L_a = 7.2$ mH, $L_f = 7.5$ mH, $K_\Phi = 1.3314$.
3) IEEE-519 limits [35]: Current distortion limits for distribution system (120 to 69 000 V) in Table I.
4) Voltage sensors: LEM made LV25P.
5) Current sensors: LEM made LA25P.
6) GSC: IGBT three-leg Semikron inverter module SKM-100GB128DN, $L_f = 4$ mH, 5 kVA star-delta transformer.
7) RSC: IGBT three-leg Semikron inverter module SKM100GB128DN.
8) Controller gains.
   a) Speed controller: $k_{pd} = 0.1$, $k_{id} = 0.12$.
   b) Current controller: k_{pdv}, $k_{pqv} = 100$, k_{idv}, $k_{iqv} = 130$.
   c) DC-link voltage controller: $k_{pdc} = 0.08$, $k_{idc} = 0.02$.

REFERENCES

[1] D. M. Tagare, Electric Power Generation the Changing Dimensions. Piscataway, NJ, USA: IEEE Press, 2011.
[2] G. M. Joselin Herbert, S. Iniyan, and D. Amutha, "A review of technical issues on the development of wind farms," Renew. Sustain. Energy Rev., vol. 32, pp. 619–641, 2014.
[3] I. Munteanu, A. I. Bratcu, N.-A. Cutululis, and E. Ceang, Optimal Control of Wind Energy Systems Towards a Global Approach. Berlin, Germany: Springer-Verlag, 2008.
[4] A. A. B. Mohd Zin, H. A. Mahmoud Pesaran, A. B. Khairuddin, L. Jahanshaloo, and O. Shariati, "An overview on doubly fed induction generators controls and contributions to wind based electricity generation," Renew. Sustain. Energy Rev., vol. 27, pp. 692–708, Nov. 2013.
[5] S. S. Murthy, B. Singh, P. K. Goel, and S. K. Tiwari, "A comparative study of fixed speed and variable speed wind energy conversion systems feeding the grid," in Proc. IEEE Conf. Power Electron. Drive Syst. (PEDS'07), Nov. 27–30, 2007, pp. 736–743.
[6] D. S. Zinger and E. Muljadi, "Annualized wind energy improvement using variable speeds," IEEE Trans. Ind. Appl., vol. 33, no. 6, pp. 1444–1447, Nov./Dec. 1997.
[7] H. Polinder, F. F. A. van der Pijl, G. J. de Vilder, and P. J. Tavner, "Comparison of direct-drive and geared generator concepts for wind turbines," IEEE Trans. Energy Convers., vol. 21, no. 3, pp. 725–733, Sep. 2006.
[8] R. Datta and V. T. Ranganathan, "Variable-speed wind power generation using doubly fed wound rotor induction machine—A comparison with alternative schemes," IEEE Trans. Energy Convers., vol. 17, no. 3, pp. 414–421, Sep. 2002.
[9] E. Muljadi, C. P. Butterfield, B. Parsons, and A Ellis, "Effect of variable speed wind turbine generator on stability of a weak grid," IEEE Trans. Energy Convers., vol. 22, no. 1, pp. 29–36, Mar. 2007.